

Evaluation Analysis of Double Coil Heat Exchanger for Heat Transfer Enhancement

Senaa Kh. Ali ¹, Itimad D.J. Azzawi ^{2*}, Anees A. Khadom ³

^{1,2}Department of Mechanical Engineering, College of Engineering, University of Diyala, 32001 Diyala, Iraq

³ Department of Chemical Engineering, College of Engineering, University of Diyala, 32001 Diyala, Iraq

ARTICLE INFO	ABSTRACT
<p>Article history: Received 8 November 2020 Accepted 5 March 2021</p> <p>Keywords:</p> <p>Double coil; Flow rate; Coil pitch; Secondary flow</p>	<p>In order to maximize the thermal efficiency of shell and coil heat exchangers, substantial research has been done and geometrical modification is one way to improve the exchange of thermal energy between two or more fluids. One of the peculiar features of coiled geometry is that the temperature distribution is highly variable along the circumferential section due to the centrifugal force induced in the fluid. Moreover, most researchers are concentrated on using a shell and single helical coil heat exchanger to enhance the heat transfer rate and thermal efficiency at different operating parameters. Therefore, the aim of this study is to investigate temperature variation ((T-1, T-2, T-3 and T-4) across a shell and single/double coil heat exchanger at different coil pitches, hot water flow rate, and cold-water flow rate along the outer surface of the coil using experimental and numerical analysis. For single and double coil heat exchangers, Computational Fluid Dynamics (CFD) is carried out using pure water with a hot water flow rate ranging between 1-2 l/min for the coil side heat exchanger. For single coil heat exchangers, the numerical analysis findings showed a good agreement with experimental four-temperature measurement results (T-1, T-2, T-3 and T-4) with an error rate of 1.80%, 3.05%, 5.34% and 2.17% respectively. Moreover, in the current double coil analysis, the hot outlet temperature decreased by 3.07% compared to a single coil (baseline case) at a 2.5L/min hot water flow rate. In addition, increasing the coil pitch will increase the contact between the hot fluid and the coil at a constant hot water flow rate and thereby decrease the hot fluid outlet temperature. Finally, a computational analysis was carried out to examine the flow structure inside single and double coil heat exchangers, and the findings indicated that the effect of centrifugal forces in double coil heat exchangers at various coil pitches caused the secondary flow to be substantially reduced.</p>

1. Introduction

As one of the passive heat transfer improvements, helically coiled tube heat exchangers have been widely researched and have applications in diverse industries: pharmaceutical, biological, petrochemical, mechanical and biomedical [1]. Different experimental and computational methods studies have conducted to analyze the effects of

secondary flow motion induced by curvature and centrifugal force in helical coils, these studies clarified the flows within helically coiled by laminar and turbulent flows [2-6]. Eustice [7] has introduced experimental study to investigate the flow within the helical coil tube made of glass and full of water, and it has been noted that the centrifugal force induces secondary flow, and this is the essence of curved flow. Later,

* Corresponding author.

E-mail address: itimaddawood_eng@uodiyala.edu.iq

DOI: 10.24237/djes.2021.14109

Dean [8] has given the first approximation of the laminar flow into an infinitely long curved pipe with a circular cross-section with a mathematical analysis used to investigate the fluid motion through a coil pipe. This effect has established to be a dimensionless quantity to describe the secondary flow magnitude, called Dean Vortices, as seen in Figure 1. It laid the basis for further studies [9,10] and greatly contributed to the understanding of the flow through curved pipe.

In order to verify the distribution of velocity, pressure field and secondary flow at various coil parameters, Lingdi et al [11] investigated the numerical efficiency of flow characteristics inside a helical coil (i.e., Dean number, curvature radius, and coil pitch). The results revealed that the velocity gradient increases in the helical coil tube and the secondary flow is the main reason for reduction of flow causing turbulent flow inside the coil.

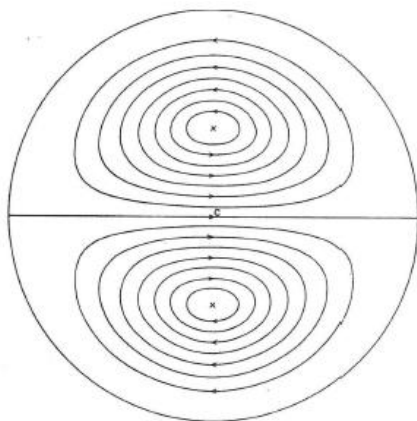


Figure 1. Flow pattern in helical coil showing the secondary flow

Anwer et al [12, 13] examine the influence of laminar flows on the coil friction factor and wall shear stress using numerical simulation at coil pitch varies from 0.01 to 0.025m. They observed that the 0.05m coil pitch was not significantly different from the 0.01m coil pitch, where the maximal pressure fell from 71 Pa for 0.01m coil pitch and 68.8 Pa for 0.05m coil pitch. Due to the extra helix length, the percentage of rise in pressure as the coil pitch increased from 0.25m to 0.05m is almost 47%. In order to demonstrate the influence of varying

coil pitch on the coil friction factor and wall shear tension, the same authors [14] performed a theoretical investigation of turbulent flow within the helical coil. Two turbulence models were used to test the turbulence model that could capture the flow characteristics (STD ($k-\epsilon$) and STD ($k-w$)). The findings revealed that the Dean number had a greater effect on decreasing the coil friction factor in turbulent flows than on increasing the pitch dimension. Moreover, a CFD analysis was used by Kumar and Chandrasekar [15] to measure the heat transfer and pressure drop under laminar flow of the double helically coiled tube heat exchanger at Dean number ranged between 1300 to 2200. The results revealed a good agreement between the CFD and the experimental findings and 7.2% and 8.5% respectively were considered to be the difference between the Nusselt number and decreased pressure. A shell and coil heat exchanger were also studied by Jayakumara [16] using both numerical and experimental analysis to investigate the effect of different coil parameters on the thermal performance. In the heat transfer forming field, the results showed that the coil pitch is important. Also, a correlation was proposed to determine the heat transfer coefficient in the coil tube.

According to the previous studies and to the best of the authors knowledge, most researchers are concentrated on using a shell and single helical coil heat exchanger to enhance the heat transfer rate and thermal efficiency at different operating parameters. Therefore, in order to examine the ability to improve the heat transfer rate by increasing the contact area of the coil surface, the current study compared single (baseline case) and double coil heat exchangers in terms of four temperatures distributed along the coil surface (T-1, T-2, T-3, and T-4). This improvement can be performed by the use of double helical coil with three different coil pitch arrangements ($p = 30, 60$ and 90), water flow rate of coil side and water flow rate of shell side. Meanwhile, to examine flow structure inside the single and double helical coil, the secondary flow output is studied with multiple Reynolds number coil side under turbulent flow.

2. Experimental work

2.1 Materials and setup

The schematic diagram and picture of the experimental setup are illustrated in Figure 2 and 3. The heat exchanger included an acrylic shell and helical coil tube made from copper. In addition, there are a variety of components in the setup for the heat exchanger: eight 22 K thermocouples (± 1.5 °C uncertainty) connected to the data logger and PC, 500 L electrically heated water, pump, ball valves and LZM flow meter (± 0.25 L/min uncertainty). The eight thermocouples were separated into four from the bottom of the coiled tube and then attached to the coil surface, while the other four were used to measure the hot water inlet and outlet $T(h, i)$ and $T(h, o)$ and the cold water inlet and outlet ($T_{co, i}$, $T_{co, o}$). The thermocouple distribution can be seen in Figure 2. The findings were recorded using an NI Compact DAQ 4 data loggers attached to a PC, and the data was analyzed using LabVIEW.

First of all, to ensure that all thermocouples (T-1, T-2, T-3 and T-4), T-(h,i) and T-(h,o) attached to the outer surface coil read the same

result, the hot water was inserted into the coil before the cold water was incorporated into the shell side such that it was noticed all thermocouples attached to the outer surface coil read the same temperature. In four cases used in the current study, the hot water flow rate and inlet temperature were maintained at 1L/min and 65 °C, respectively. To avoid heat loss and to maintain hot water at the appropriate temperature, a 4 cm thick sheet of laminated glass wool was used as a thermal insulator around the storage tank. Where the hot water from the water storage tank 500 L was supplied for the coil side, and this water would be returned to the storage tank from the coil for reheating. The cold water is pumped into the shell side with variable flow rates ranging from 2 - 8 L/min with an inlet temperature of 36 °C through the heat exchanger's base. For the control of the flow rate on both sides, two ball valves were used.



Figure 2. Model design and experimental set-up

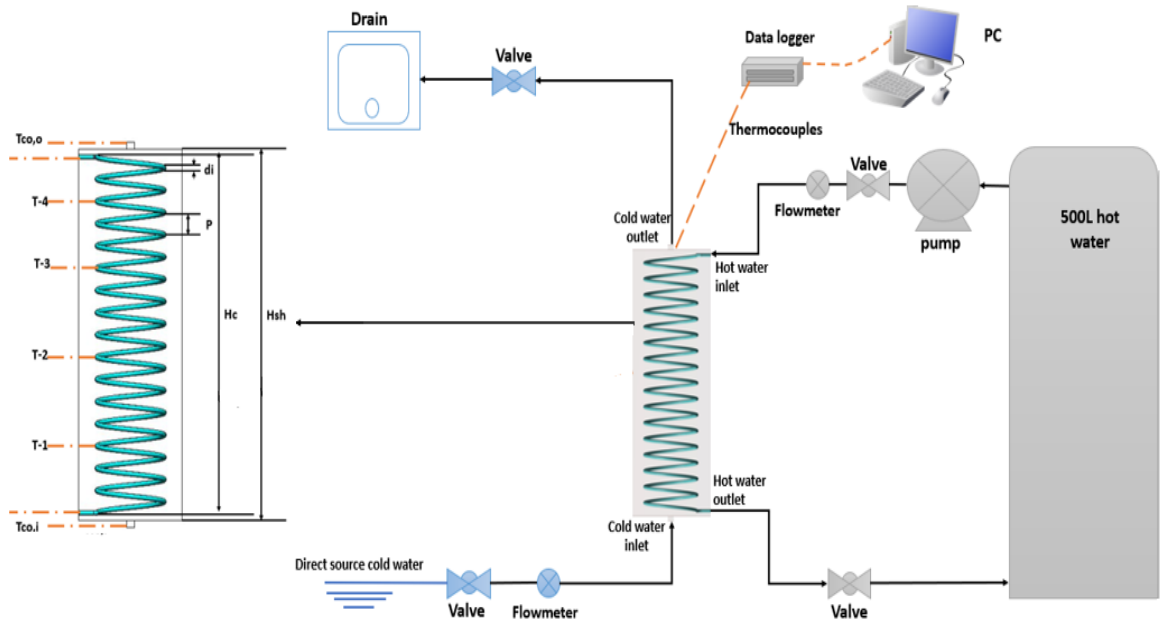


Figure 3. Schematic diagram of the experimental set-up

3. Numerical study

Figure 4 shows the vertical shell configuration with double coil heat exchanger. The shell and helical coil heat exchanger was designed and transferred to ANSYS in order to measure the temperature distribution along the coil surface (T-1, T-2, T-3 and T-4). Moreover, the single coil was modified into double coil to make eight turns for each coil, keeping the first coil diameter (curvature diameter) constant at

$D_{c1}=114$ mm with the second double coil diameter (D_{c2}) modified many times (i.e., $D_{c2} = 57, 95, 130, 140$ and 150 mm). As it was mentioned in the previous research [17], the appropriate position of the second curvature diameter at 150 mm produces the optimum heat transfer rate. Therefore, a double coil with a second coil curvature diameter of 150 mm was selected in this research at coil pitch 60 mm. Figure 5 depicts the dimensions of single and double coil heat exchangers.

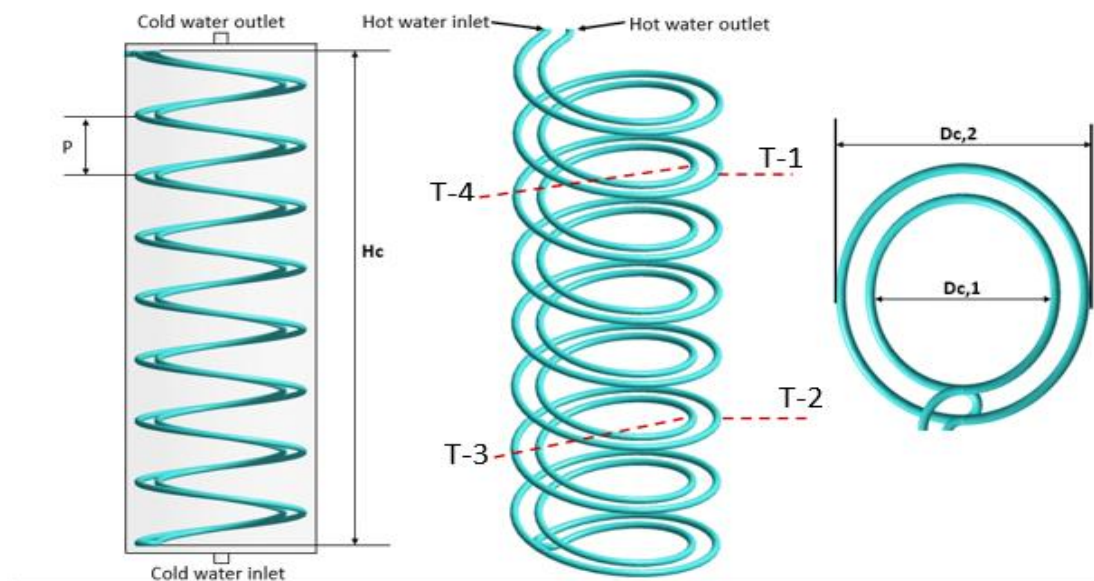


Figure 4. Schematic of the shell and double coil heat exchanger

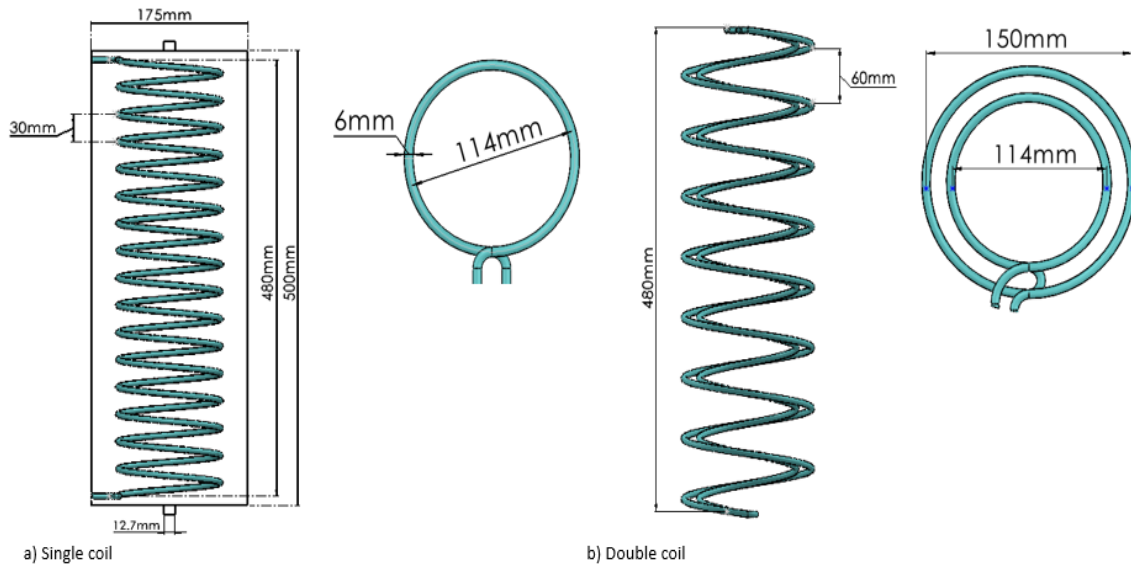


Figure 5. The design of single and double coil heat exchanger

3.1 Mesh independency check

Due to the complicated structure of the shell and coil heat exchanger, the shell and coil domain were meshed with tetrahedral meshes. Also, the mesh at some regions was refined such as the inlet and outlet of the shell and the relatively close region of the outer surface of the coil as show in Figure 6. In order to validate the precision of the numerical results, Mesh

independency study was performed by applying six different numbers of grids. Figure 7 indicates the hot and cold temperature outlet determined by the six grid systems for the coil and shell sides, and the 1657963 grids scheme is suitable for grid independent solutions. Therefore, the 1657963 grids were used in the current study because further mesh refining has no significant effect on the monitoring values.

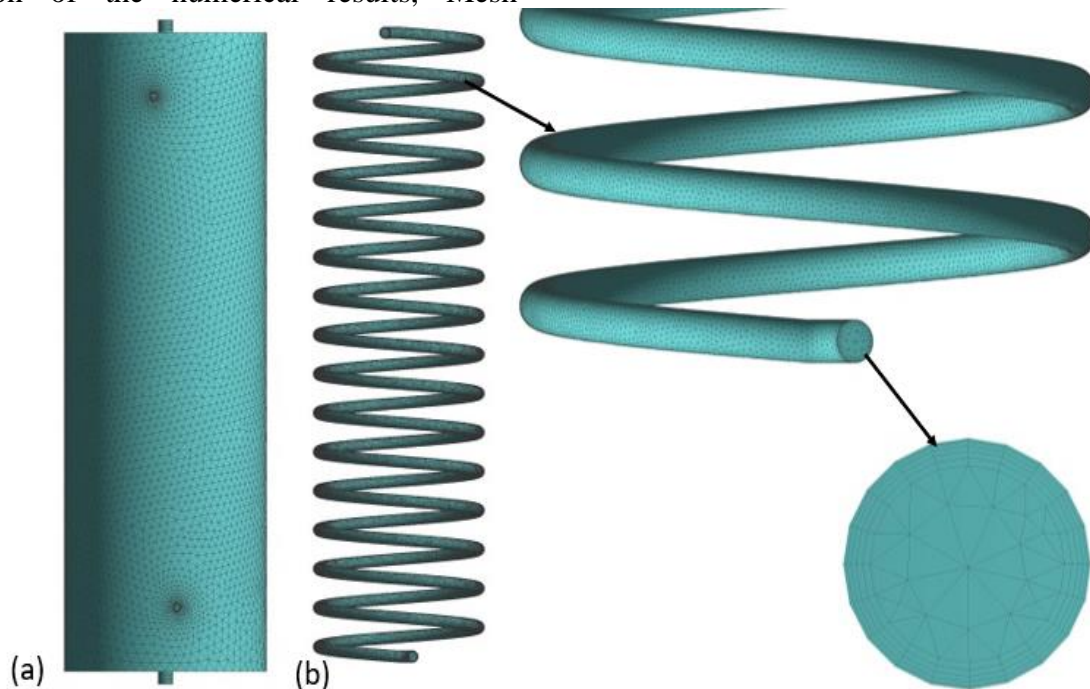


Figure 6. Generated mesh for a) Shell side, b) Coil pipe

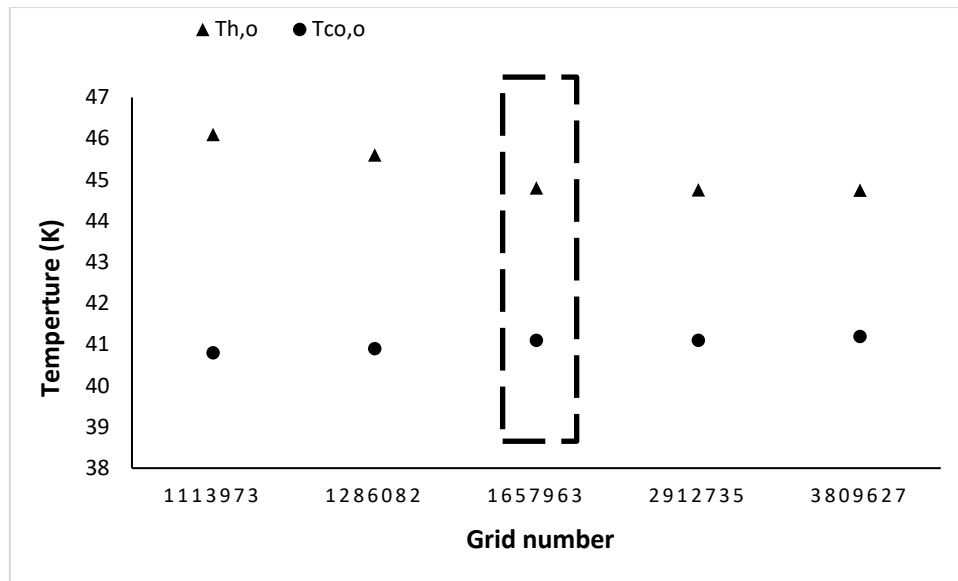


Figure 7. Mesh sensitivity analysis temperature vs grid number

3.2 Governing equations, boundary condition and assumptions

The numerical analysis was carried out 3D at steady state with solving the governing equations include continuity, momentum, and energy equations [18]. The section provides these equations:

Continuity equation:

$$\frac{\partial}{\partial x_i}(\rho u_i) = 0 \quad (1)$$

Momentum equation:

$$\frac{\partial}{\partial x_j}(\rho u_j u_i) = -\frac{\partial p}{\partial x_i} + \frac{\partial \tau_{ij}}{\partial x_j} \quad (2)$$

Energy equation:

$$\frac{\partial}{\partial x_j}(\rho u_j (\theta + \frac{1}{2} u_j \tau_{ij})) = \frac{\partial}{\partial x_j} (u_i \tau_{ij}) + \frac{\partial}{\partial x_j} (k \frac{\partial T}{\partial x_j}) \quad (3)$$

where τ_{ij} is the viscous stress tensor defined as follows:

$$\tau_{ij} = 2\mu S_{ij} \quad (4)$$

S_{ij} is the strain rate tensor which can be written as:

$$S_{ij} = \frac{1}{2} \left(\frac{\partial u_i}{\partial x_j} + \frac{\partial u_j}{\partial x_i} \right) \quad (5)$$

whereas to simulate turbulent flow the RNG k- ϵ turbulence model was used [16].

Turbulent kinetic energy k:

$$\frac{\partial}{\partial x_i}(\rho k u_i) = G_k + \frac{\partial}{\partial x_j} \left(\alpha_k \mu_{eff} \frac{\partial k}{\partial x_j} \right) - \rho \epsilon \quad (6)$$

Energy dissipation rate ϵ :

$$\frac{\partial}{\partial x_j}(\rho \epsilon u_j) = \frac{\partial}{\partial x_j} \left(\alpha_\epsilon \mu_{eff} \frac{\partial \epsilon}{\partial x_j} \right) + C_{1\epsilon} \frac{\epsilon}{k} G_k - \rho C_{2\epsilon} \frac{\epsilon^2}{k} - R_\epsilon \quad (7)$$

The boundary conditions were set as shown in Table 1 with a constant temperature of 36 °C for cold water and 65 °C for hot water.

The inlet boundary condition was set as the mass flow rate for cold and hot water, the outlet boundary condition was select as pressure outlet with zero back flow pressure. In addition, to solve the coupling between pressure and velocity fields, the Basic (Semi Implicit Method for Pressure Related Equations) algorithm was used. For discretization pressure, momentum, energy and RNG k- ϵ turbulence equations, the first-order upwind system was used. Moreover, Only the cold-water flow rate (shell side) was varied due to the experimental limitation of the hot water flow rate that reaches the coil side. However, the hot water flow rate used in the numerical simulation (coil side) can be adjusted if desired, therefore, the hot water flow rate was varied from 1 to 2.5 L/min for single and double coils with a constant cold-water flow rate of 2 L/min which can be used to study the effect on hot outlet temperature.

Table 1: Boundary conditions for validation and numerical analysis

Parameters	Shell side	Coil side
Working fluid	cold water	Hot water
Material	acrylic	Copper
Inlet temperature	36 °C	65 °C
Inlet (mass flow rate kg/s)	0.0333 – 0.1331	0.01664 – 0.0416
Outlet	Pressure outlet	Pressure outlet
wall	No slip No heat flux	Coupled

4. Results and discussions

4.1 Numerical simulation validation

Validation of the Numerical model developed in ANSYS Fluent was done by comparing the Numerical results for temperature along the outer surface of the coil (T_1, T_2, T_3 and T_4) with that obtained from experimental data. As shown in Figure 8, the numerical results with experimental results for the temperatures (T_1, T_2, T_3 and T_4) are in good agreement within an error of 1.80%, 3.05%, 5.34% and 2.17% respectively.

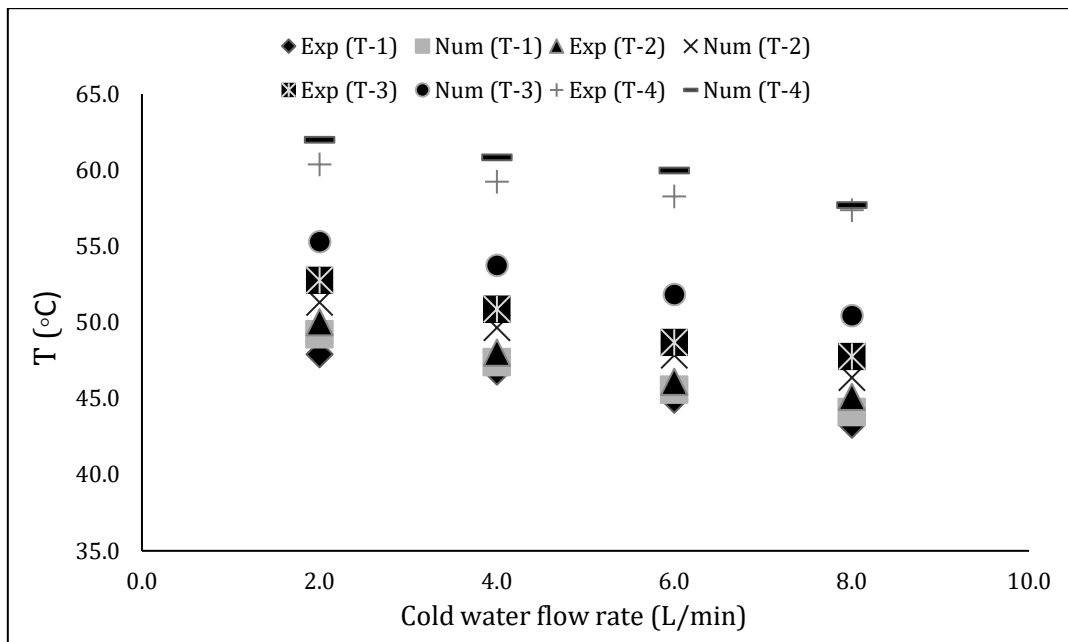


Figure 8. Comparison between the numerical simulation and experimental results of shell side flow rate vs temperature

4.2 Comparison between single (baseline case) and double coils

The effect of the second coil curvature diameter ($D_{c2}=150\text{mm}$) on the temperature distribution along the outer surface of the coil was numerically investigated. Results of this section have obtained for various hot water flow rate and constant cold-water flow rate as shown in Table 1. According to the Figs. 9a-e, increasing the hot flow rate (coil side) with the same cold flow rate (shell side) (2L/min) increases the hot outlet temperature and the temperature distribution along outer coil surface (T_1, T_2, T_3 and T_4) for single and double coil. The figures clearly demonstrate that increasing

the hot flow rate by retaining a constant cold flow rate contributes to a reduction in the heat exchange between hot water and cold water (shell side). This is due to the short period of time when hot water comes into contact with cold water.

In comparison, the hot outlet temperature of hot fluid $T(h, o)$ and temperature ($T-1, T-2, T-3$ and $T-4$) decreased in the double coil by 3.07%, 3.01%, 2.14%, 2.25% and 2.64% respectively from the single coil (baseline case) at 2.5 L/min hot water flow rate. The lower temperatures in the double coils more than the single (baseline case) is owed to the change in coil pitch from 30mm to 60mm [19]. The coil

pitch was changed to 60 mm after it was 30 mm in the single coil to occupy the same coil height inside the shell while turning a single coil into a double coil. Therefore, a double coil was studied

at 30 mm pitch coil, its height was 240 mm inside the shell, then compared to the double coil at 60 mm and 90 mm coil pitch.

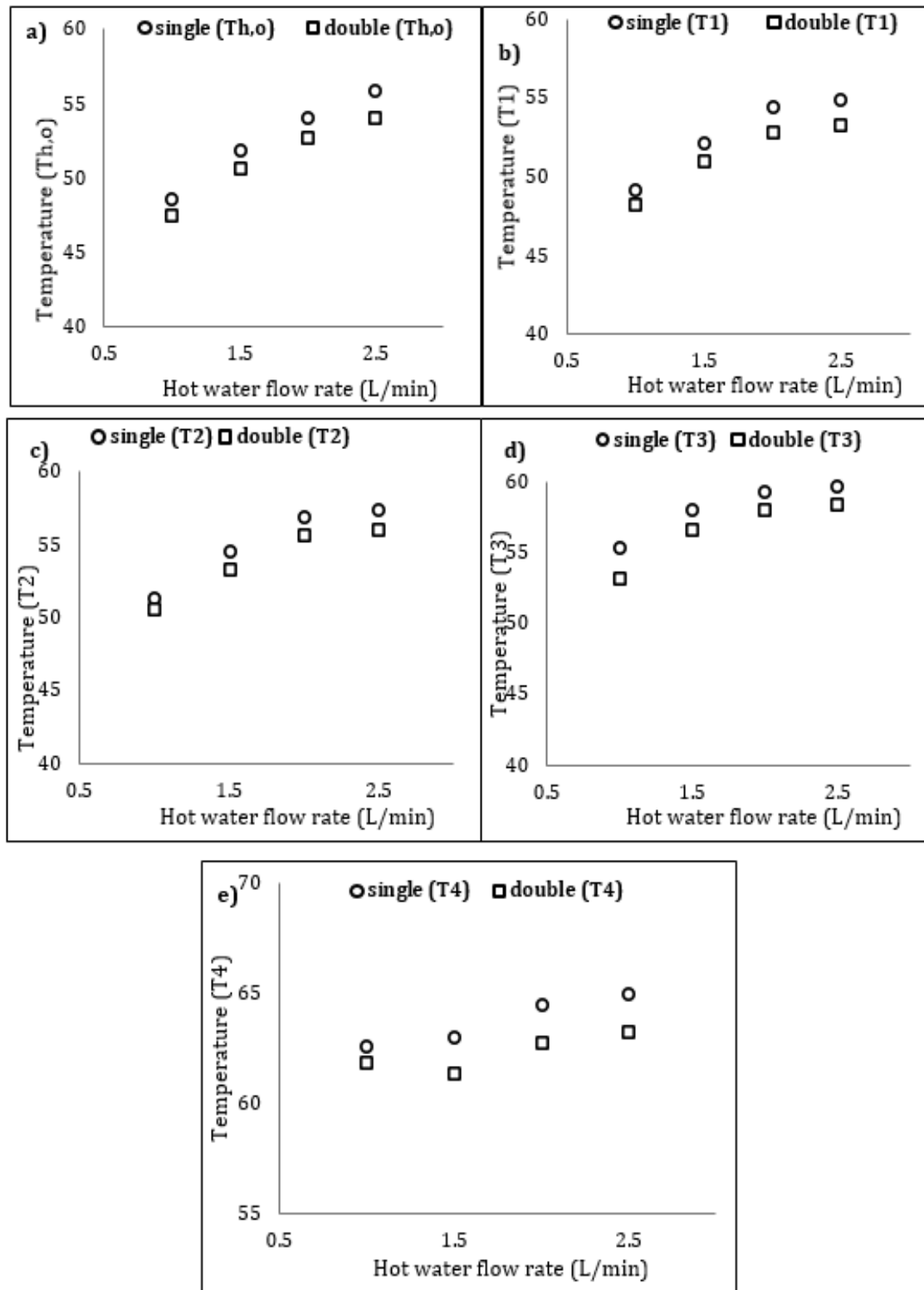


Figure 9. Variation of hot flow rate against temperature between single and double coil at cold flow rate 2 L/min. a) outlet temperature hot fluid $T_{h,o}$. b) T_1 . c) T_2 . d) T_3 . e) T_4 .

4.3 Effect of Coil Pitch

This section addresses the effects of different coil pitches on the temperature of the heat exchanger. The schematics of models studied that have different coil pitches are shown in Figure 10. The geometrical dimensions of the shell and the double coil heat exchanger are constant, and the coil pitch is varied from 30 mm to 90 mm as seen in Table 1.

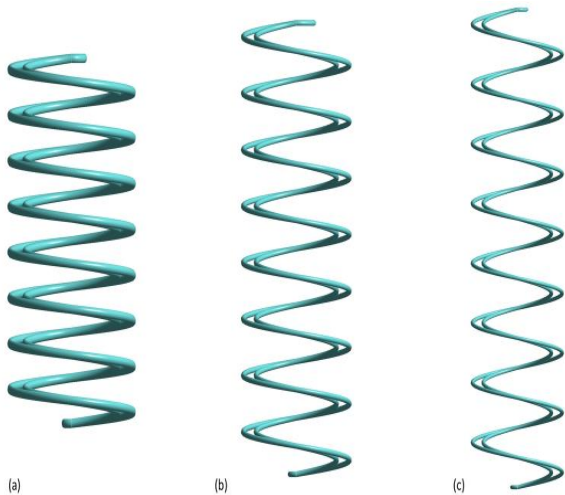


Figure 10. Studied models with different coil pitch a) P=30mm b) P=60mm c) P=90mm.

Increasing the hot-water flow rate in a constant coil pitch increases the temperature as explained in Figure 11. The figure also shows that the hot fluid outlet temperature of P= 90 mm coil pitch was reduced by 4.80% relative to the other two pitch numbers. Since the hot fluid outlet temperature drops at P= 90 mm by 2.84% and 2.16% compared to the hot fluid outlet temperature at p= 30 mm and 60 mm, respectively. Moreover, by increasing the coil pitch at a constant flow rate, the temperature of the hot fluid outlet was decreased. This is because that if the coil pitch increases, stronger interaction takes place between the hot fluid and the coil suggesting that the heat transfer between the hot and cold fluids strengthens, resulting in a drop in the temperature of the hot fluid outlet at the 90 mm coil pitch. It has been suggested that one of the reasons for the decrease in the temperature at P = 90 mm coil pitch is a shell height change from 500 mm to 780 mm, resulting in the fluid lingering within the heat exchanger long before leaving.

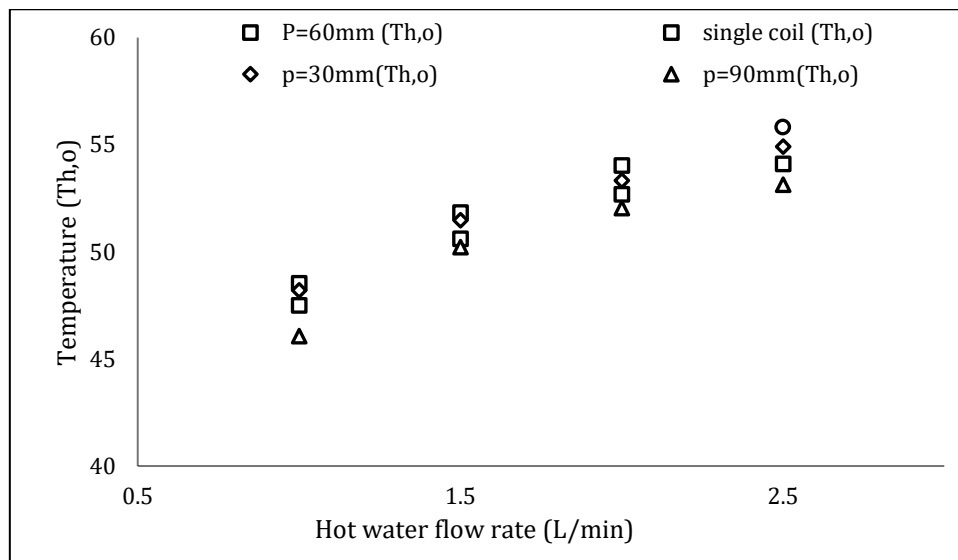


Figure 11. Variation of hot flow rate against outlet hot fluid temperature for single and double coil at cold flow rate 2 L/min

Figures. 13a-c introduce the velocity distribution at different coil pitches using various planes at different locations on the coil side (see Figure 12) with different hot water flow rate (1, 1.5 and 2 L/min). It is observed from the figures that the lower velocity near to

the wall is subject to non-slip boundary conditions and the velocity of the moving fluid (water) starts to rise from the inner wall to the outer wall. Moreover, as the velocity increased due to the centrifugal force, the effect of the curved pipe allows the secondary flow to be

generated. A pair of counter-rotation vortices are produced that force the high velocity moving fluid to the outer edge of the tube and the slower-moving fluid to the inner side of the tube, allowing the distribution of velocity to be irregular. However, the velocity contours between single and double coils appear very different. It can be seen that despite the use of different Reynolds number to achieve the distribution of velocity that has an effect on the structure of Dean vortices in double coils, the impact of a centrifugal forces in double coil at different coil pitch (30, 60 and 90 mm) causing the secondary flow significantly decreased. This is due to an increase in curvature diameter, which is proportional to the dean number in the opposite direction ($De = Re (d_i/D_c)$). Therefore, the flow structure within a helical coil is influenced by the coil pitch and curvature diameter.

Owing to the geometry of a double coil, the explanation for the difference in temperature between a single and double coil might be because counter flow between the hot and cold fluid occurs in a single coil. But a counter flow

between hot and cold fluid occurs in a double coil in the first coil, while a parallel flow between hot fluid and cold fluid occurs in the second coil. In comparison, relative to a single coil, the surface area of the double coil is expanded by 0.5 m, which helps heat transfer to be enhanced.

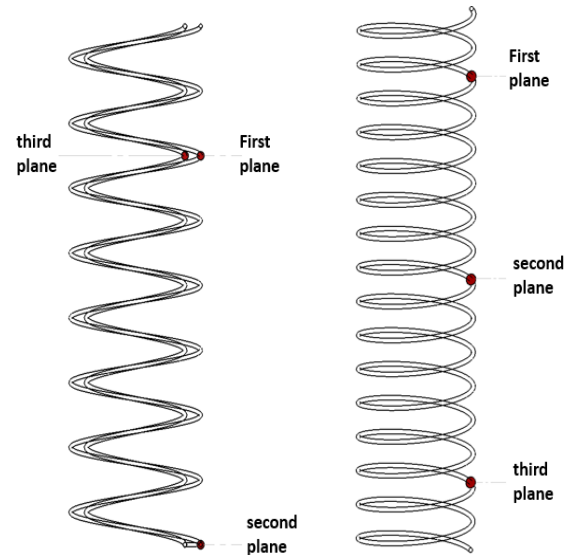
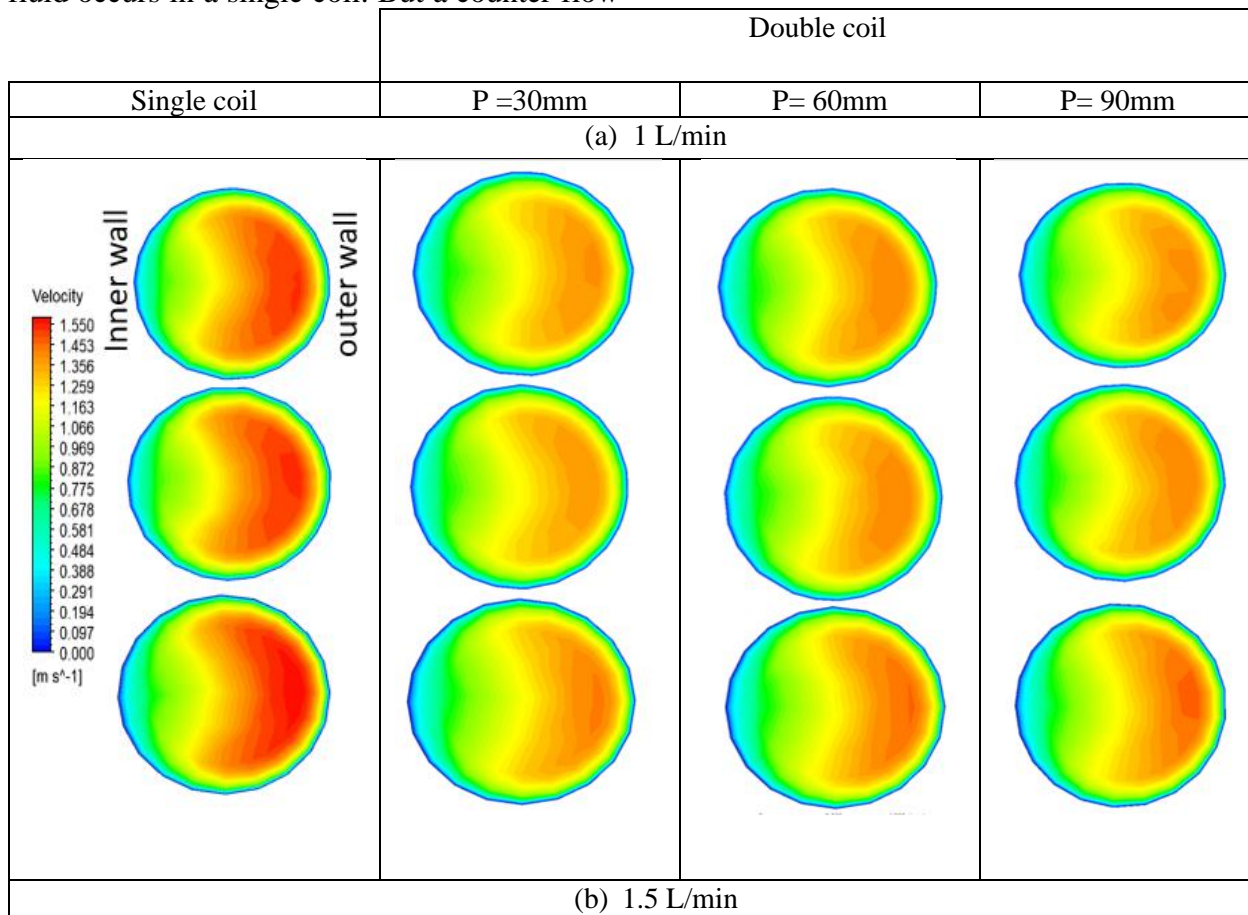


Figure 12. Plane positions for single and double coils



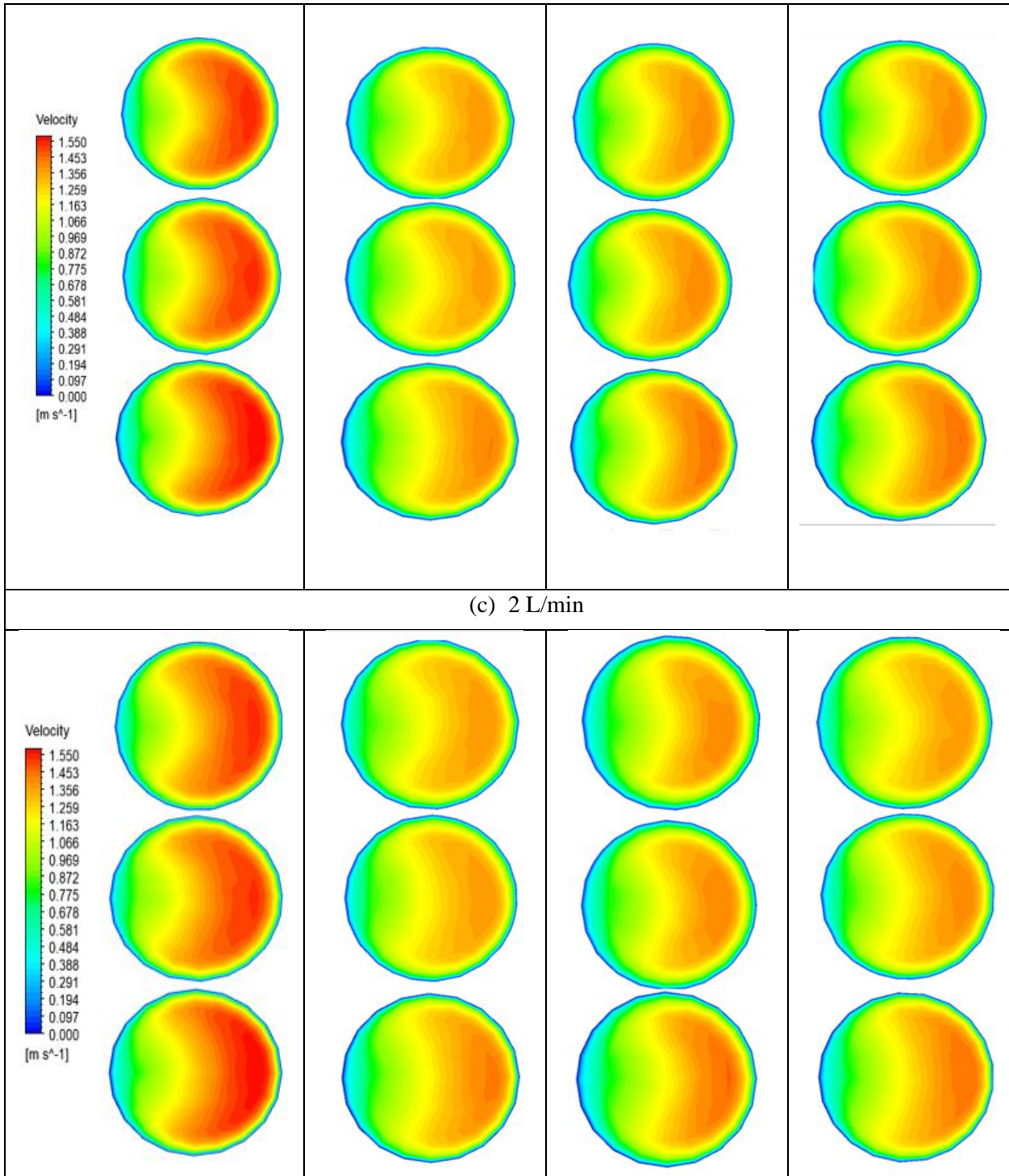


Figure 13. Various plane velocity contours for single and double coils at various hot water flow rates a) 1L/min, b) 1.5 L/min and c) 2 L/min

5. Conclusions and future work

An experimental validation and numerical investigation are provided in the present study for a shell and single/double coil heat exchanger and the effect of operating parameters (hot and cold flow rate) on the hot outlet temperature and

temperature distributed along coil surface (T-1, T-2, T-3 and T-4) has studied. The experimental and numerical findings showed that the four temperatures (T-1, T-2, T-3, and T-4) were in good agreement. According to the findings of this study, when a single coil is converted into a double coil, the hot outlet temperature and the

temperature distributed along the coil surface decreases at high hot water flow rate (2.5 L/min). Also, the results showed that the influence of coil pitch 30, 60 and 90 mm on a double coil heat exchanger was found to have a minimum temperature of 4.80% at $p = 90$ mm compared to the other two pitch numbers. In addition, the coil parameters (coil pitch and curvature diameter) have a significant impact on secondary flow within the coil. Future research can quantify LMTD and NTU to evaluate shell and double coil heat exchangers.

References

- [1] Muhammad Usman Sikandar, "Design of Helical Coil Heat Exchanger for a mini Powerplant," *International Journal of Scientific & Engineering Research* 10, (2019).
- [2] S. Liu, J.H. Masliyah, "Axially invariant laminar flow in helical pipes with a finite pitch," *J. Fluid Mech.*, (1993): 251-315.
- [3] Ashkan Alimoradi, "Investigation of exergy efficiency in shell and helically coiled tube heat exchangers," *Case Studies in Thermal Engineering* 10, (2017):1-8. <https://doi.org/10.1016/j.csite.2016.12.005>
- [4] Ahmed F. Hasan, Syed Tauseef Hossain, "Numerical Investigation of Heat Transfer Rate in Helically Coiled Pipe Using Al₂O₃/Water Nanofluid," *Diyala Journal of Engineering Sciences* 13, (2020):27-36. <https://doi.org/10.24237/djes.2020.13404>
- [5] Hüttl, T.J., Friedrich, R., "Influence of curvature and torsion on turbulent flow in helically coiled pipes," *International Journal of Heat and Fluid Flow*, 21, (2000):345-353. [https://doi.org/10.1016/S0142-727X\(00\)00019-9](https://doi.org/10.1016/S0142-727X(00)00019-9)
- [6] E. Ahmadlo, N. Sobhanifar, F.S. Hosseini, "Computational fluid dynamics on water flow through hollow helical pipe," *Open J. Fluid Dyn.* 4, (2014):133–139.
- [7] Eustice J., "Experiments on stream-line motion in curved pipes," *P R Soc Lond A: Conta.* 85 (1911):131–199.
- [8] Dean WR., "Note on the motion of fluid in a curved pipe," *Philos Mag* 4, (1927):208–233.
- [9] P.C. Mukesh Kumar and M. Chandrasekar, "A review on helically coiled tube heat exchanger using nanofluids," *Materials Today: Proceedings* 21, (2020)137-141. <https://doi.org/10.1016/j.matpr.2019.04.199>
- [10] Yanlin Zhao, Yanzhi Wang, Jun Yao, "Effect of turbulence-driven secondary flow on particle preferential concentration and clustering in turbulent square duct flows," *Particuology* 55, (2021):70-83. <https://doi.org/10.1111/j.1471-0528.1929.tb06696.x>.
- [11] Lingdi Tang, Yue Tang and Siva Parameswaran, "A numerical study of flow characteristics in a helical pipe," *Advances in Mechanical Engineering* 8, (2016):1-8. [DOI: 10.1177/1687814016660242](https://doi.org/10.1177/1687814016660242).
- [12] Anwer F. Faraj, Itimad D.J. Azzawi and Samir G. Yahya, "Investigate the Effect of Pitch Variations on Helically Coiled Pipe for Laminar Flow Region Using CFD," *International Journal of Heat and Technology* 38, (2020): 447-456.
- [13] Faraj, A. F. F., Azzawi, I. D. J., Yahya, S. G., and Al-Damook, A. "Computational Fluid Dynamics Investigation of Pitch Variations on Helically Coiled Pipe in Laminar Flow Region." *ASME. J. Heat Transfer* 142, no. 10 (2020) 104-503. <https://doi.org/10.1115/1.4047646>.
- [14] Anwer F. Faraj, Itimad D.J. Azzawi and Samir G. Yahya, "Pitch Variations Study on Helically Coiled Pipe in Turbulent Flow Region Using CFD," *International Journal of Heat and Technology* 38, (2020):775-784.
- [15] Rajesh Kumar and Prakash Chandra, "Thermal analysis, pressure drop and exergy loss of energy efficient shell, and triple meshed helical coil tube heat exchanger," *Energy Sources, Part A: Recovery, Utilization, and Environmental Effects*, (2019):1556-7036. <https://doi.org/10.1080/15567036.2019.1602213>.
- [16] J.S. Jayakumar, S.M. Mahajani, J.C. Mandal, P.K. Vijayan and Rohidas Bhoi, "Experimental and CFD estimation of heat transfer in helically coiled heat exchangers," *chemical engineering research and design* 86, (2008): 221–232.
- [17] Senaa Kh. Ali, Itimad D.J. Azzawi and Anees A. Khadom, "Experimental validation and numerical investigation for optimization and evaluation of heat transfer enhancement in double coil heat exchanger," *Thermal Science and Engineering Progress* 22, (2021). <https://doi.org/10.1016/j.tsep.2021.100862>.
- [18] Ashkan Alimoradi and Meysam Maghareh, "Numerical investigation of heat transfer intensification in shell and helically coiled finned tube heat exchangers and design optimization," *Chemical Engineering and Processing: Process Intensification* 121, (2017): 125-143.
- [19] Mehdi Noorbakhsh, Seyed S. M. Ajarostaghi, Mohsen Pourfallah and Mohammad Zaboli, "Numerical evaluation and the effects of geometrical and operational parameters on thermal performance of the shell and double coil tube heat exchanger," *heat transfer* 49, no. 8 (2020): 4678-4703. <https://doi.org/10.1002/htj.21847>.